
Quarterly Progress Report for the period November 1, 2004 –January 31, 2005

Report #13 January 31, 2005

Patrick A. Tresco, P.I.

Keck Center for Tissue Engineering

Department of Bioengineering

University of Utah

Subcontract for N01-NS-1-2338

OVERVIEW

The following report is a summary of our activity in the 13th quarter of our contract. We discuss in vivo studies that compared the brain tissue reaction to microelectrode arrays in different rat strains and report on our progress examining chronic brain tissue response to microelectrodes at 4 and 12 weeks.

In our previous report we compared microglial cytokine release on materials of widely differing surface chemistry and found that modest changes in microelectrode surface chemistry were unable to modulate the functional state of activated microglia in vitro. We concluded that any material surface that permits microglial cell attachment will likely lead to proinflammatory and profibrogenic cytokine release. Moreover, we found significant differences in microglial cytokine release when we examined cells isolated from outbred and inbred rat strains. Activated microglia derived from outbred Sprague-Dawley rat cerebral cortices released significantly more pro-inflammatory and cytotoxic cytokines than analogous cells derived from the Fischer 344 strain. The results suggested that the rat strain used for implantation studies may have a marked effect on the tissue response observed and may be an important factor in selecting an appropriate preclinical animal model. Toward this end, we compared the brain tissue reaction to implanted microelectrode arrays in male Fischer 344 rats and male Sprague-Dawley rats. So far, our analysis indicates that the overall pattern of reactivity is similar in that ED-1 immunoreactivity dominates the interface and is surrounded by and upregulation of GFAP. At the brain tissue interface there is also loss of neurofilament and NEUN immunoreactivity indicating a loss of nerve cells. Overall the pattern of reactivity appears greater in the Sprague-Dawley strain than in the Fischer 344s, in a manner that parallels our in vitro cytokine release studies. Animals that have been implanted at 4 weeks and 12 weeks are still being analyzed.

To gain insight into the longer term brain tissue reaction to implanted silicon microelectrode arrays much of the remainder of our efforts this quarter have been spent preparing animals for analysis of longer indwelling times. This quarter we have implanted animals with the following types of implants including uncoated silicon microelectrode arrays in cortex of Fischer 344s for 12 weeks (N=12); uncoated silicon microelectrode arrays in cortex of Sprague Dawleys for 12 weeks (N=12); Alginate coated silicon microelectrode arrays in cortex of Fischer 344s for 4 weeks (N=6) and 12 weeks (N=6); Alginate-NGF coated silicon microelectrode arrays in cortex of Fischer

344s for 4 weeks (N=6) and 12 weeks (N=8). These experiments are in various stages of analysis and will be presented in the next quarterly report or as they are completed.

Methods:

Alginate coatings: Alginate and alginate-NGF releasing coatings were applied by the Martin group as described in the Michigan portion of previous progress reports.

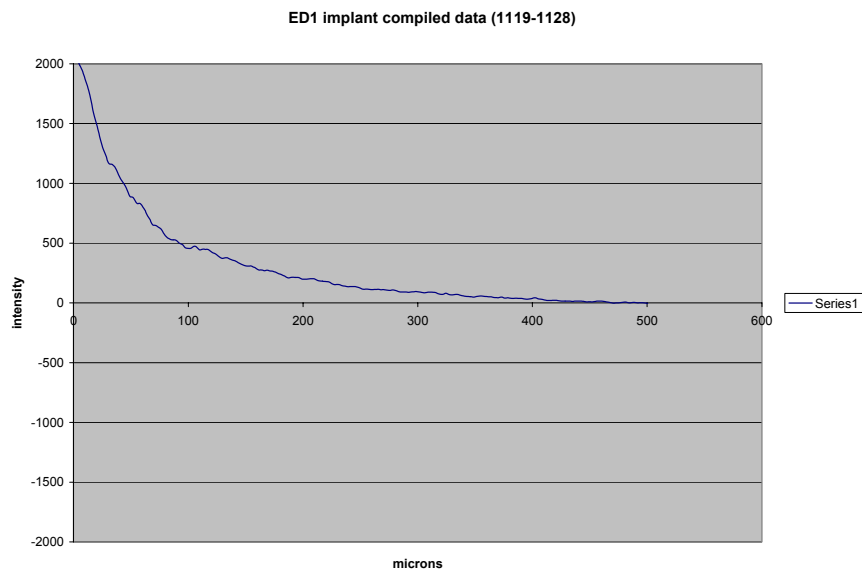
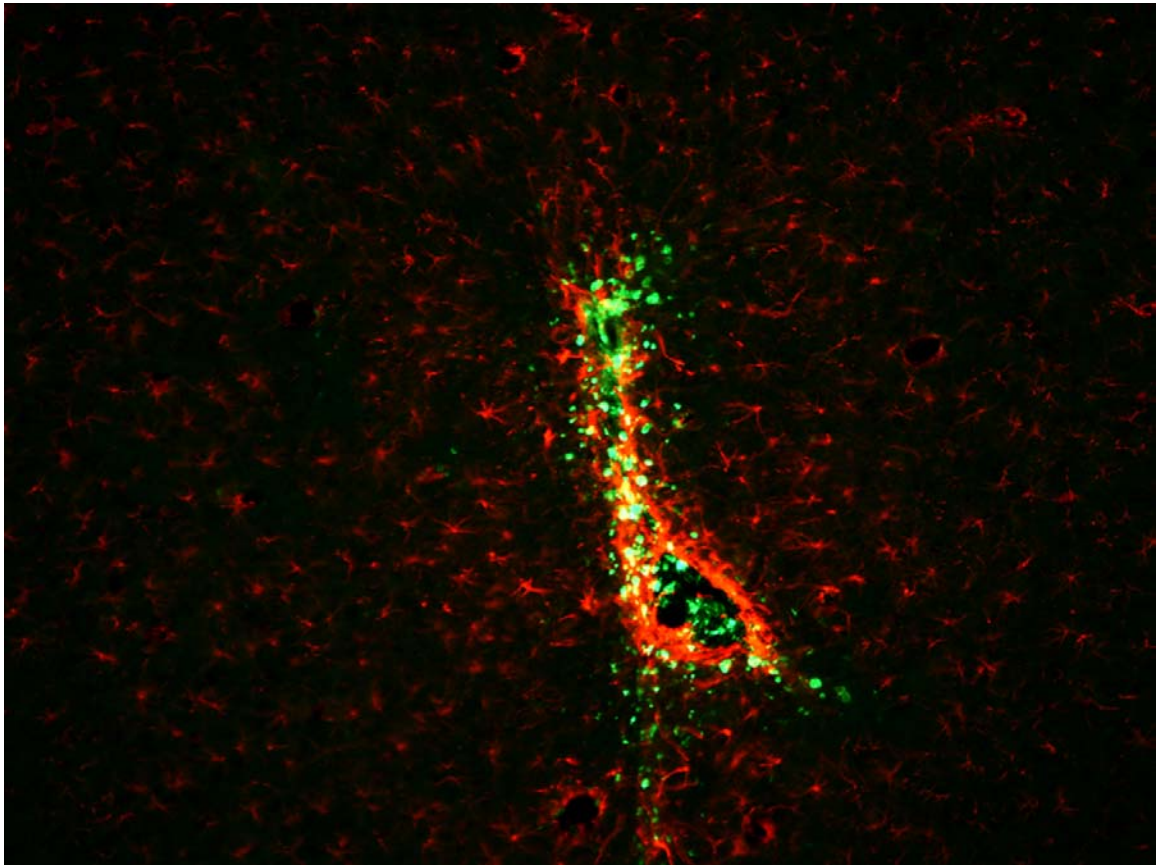
Implantation of electrodes: As previously described.

Tissue processing and immunohistology: As previously described.

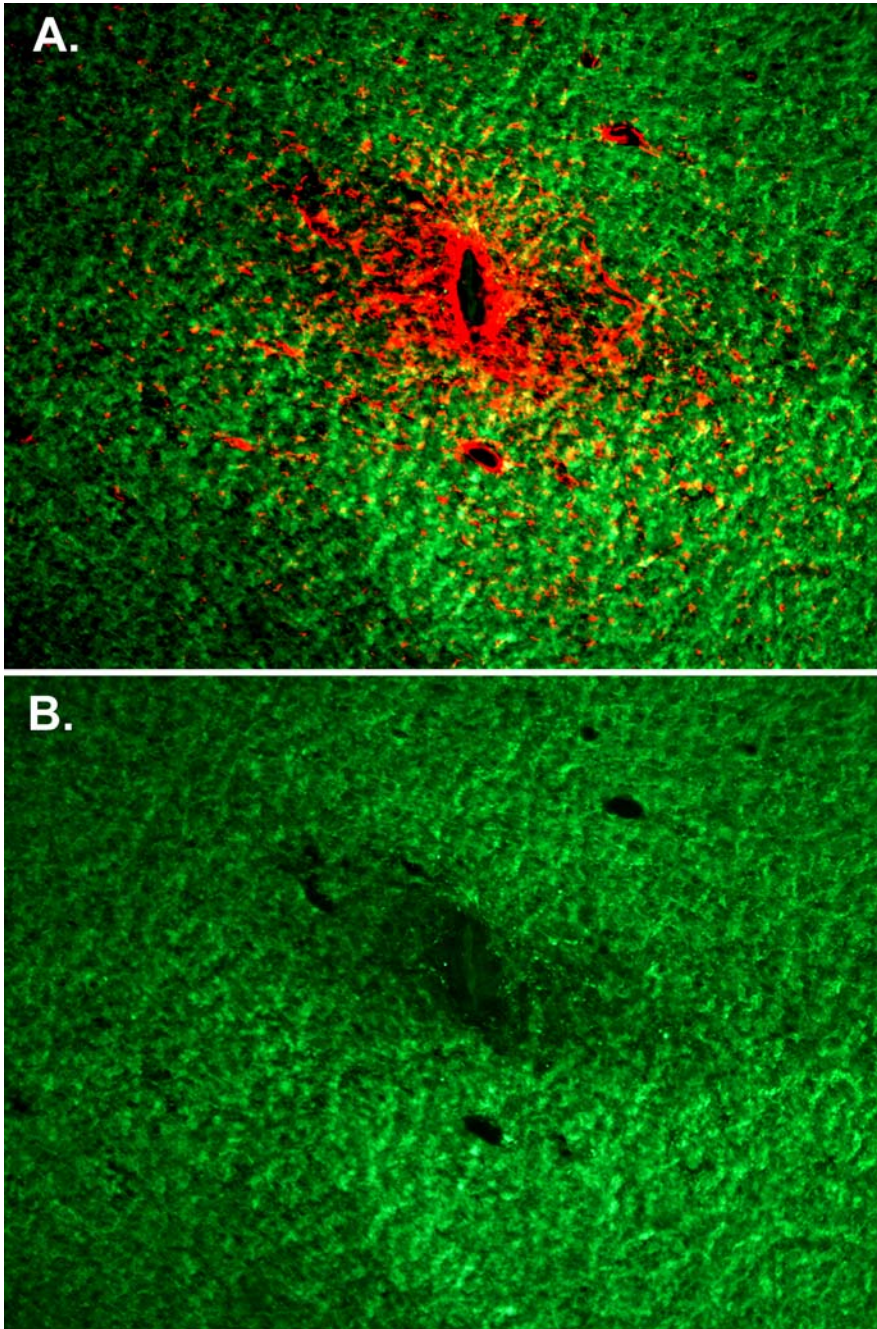
Results:

Neuronal cell loss is observed adjacent to implanted silicon microelectrode arrays in Sprague Dawley rats indicating that our earlier observations of brain reactivity to implanted microelectrode arrays was not strain dependent. Moreover, the pattern of reactivity appears greater in the outbred strain.

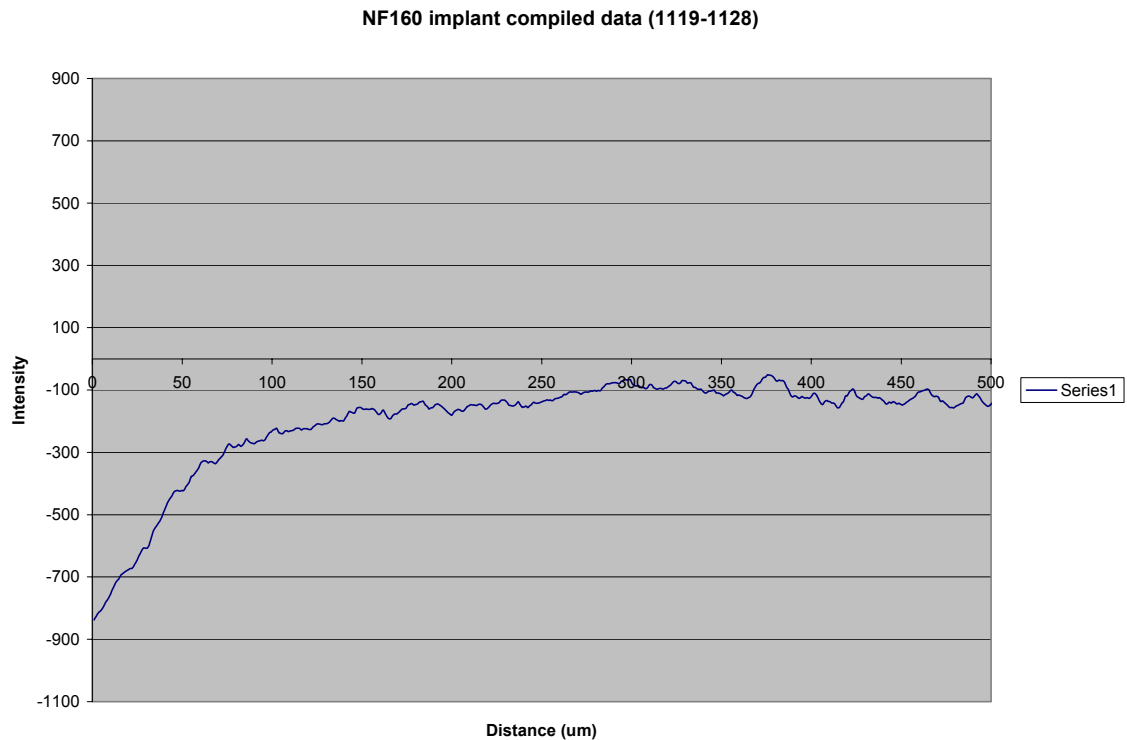
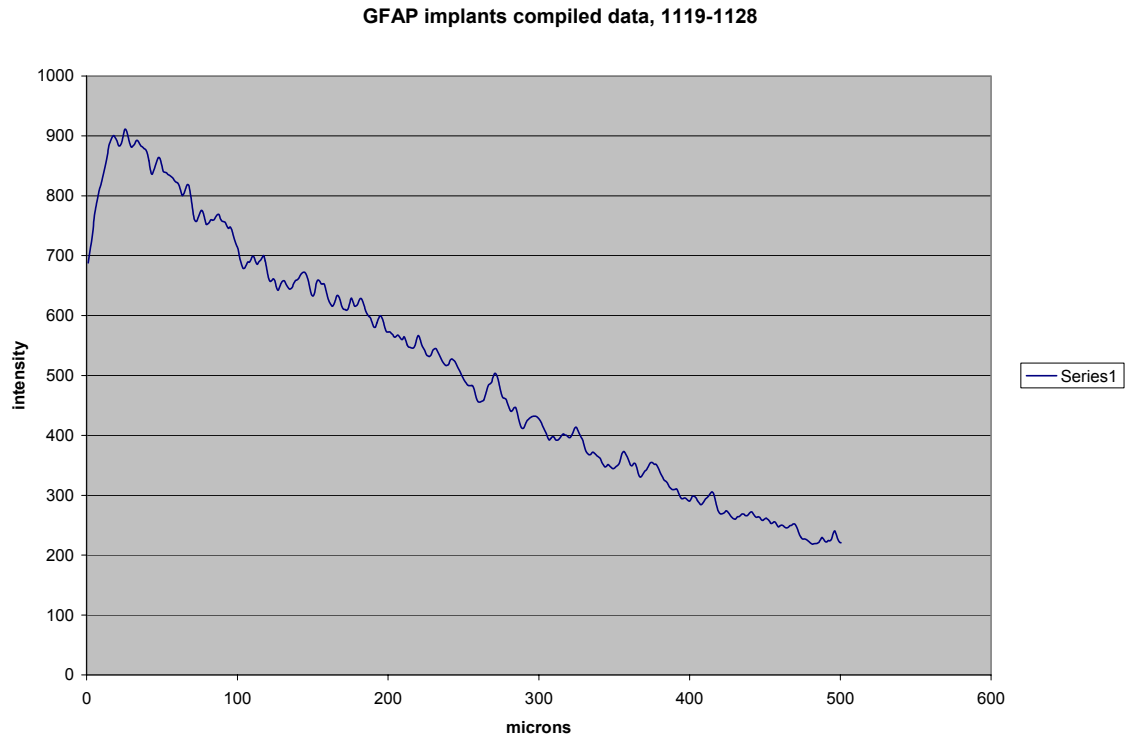
Accompanying the accumulation of ED-1 immunoreactivity at the electrode-brain tissue interface is a marked decline in the density of neuronal fibers and neuronal cell bodies in the adult rat motor cortex of the Sprague-Dawley rats (Fig. U13-1 upper panel). This is supported by a quantitative analysis of ED-1 immunolabeling as measured from multiple animals as previously described (Fig. U13-1 lower panel). Figure 13-2 shows the general pattern of GFAP immunoreactivity in horizontal sections as well as the pattern of loss of neurofilament staining, while figure 13-3 summarizes the quantitative analysis of GFAP and NF immunoreactivity. In some animals we have observed reductions in neurofilament immunoreactivity as far away as 300 microns from the electrode extending into the adjacent brain tissue (Figure U13-2). Neuronal loss at 2 weeks can also be observed with NeuN⁺ immunostaining and appears greatest in areas of increased ED-1 immunoreactivity. This reduction is not a direct result of the initial penetrating injury during implantation, as we observed little or no neurofilament loss in silicon microelectrode stab controls. In contrast, the data clearly demonstrate a reduction in neuronal density surrounding chronically implanted microelectrode that is associated with the continued presence of the foreign body. Retrieved silicon microelectrode arrays from Sprague Dawley rat motor cortex as observed with those retrieved from the motor cortex of Fischer 344s were covered with ED-1+ cells. Overall the pattern of cortical reactivity to implanted passive silicon microelectrode appears greater in the Sprague Dawley brain compared to the same region in the Fischer 344.



U13-1: Representative horizontal section through the microelectrode tract in motor cortex of young adult male Sprague Dawley showing the spatial distribution of GFAP (red) and ED-1 (green) at the microelectrode brain tissue interface 2 weeks after implantation (upper panel). Quantitative analysis of ED-1+ immunoreactivity as a function of distance from the microelectrode brain tissue interface (lower panel).

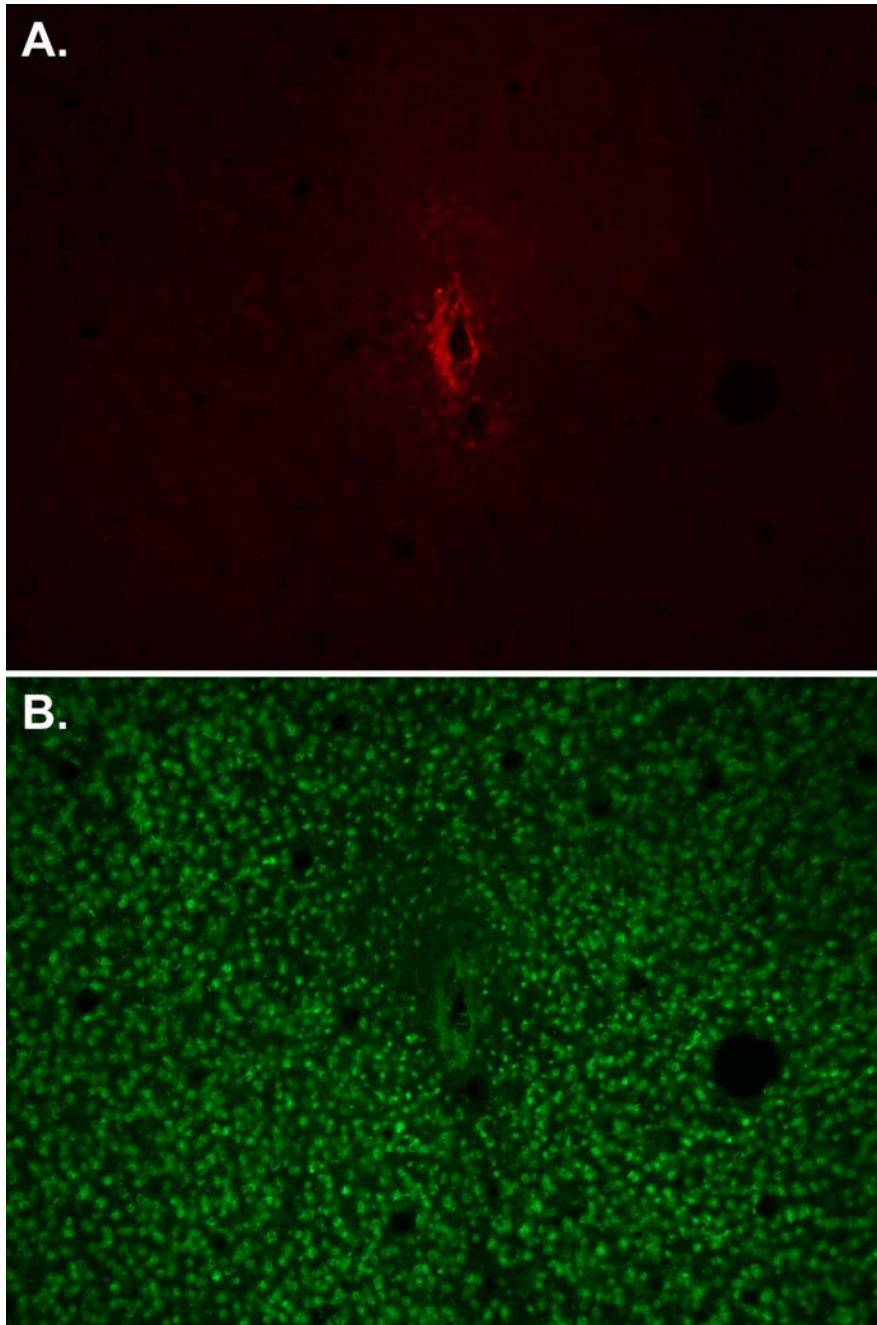


U13-2: Representative horizontal section through the microelectrode tract in motor cortex of young adult male Sprague Dawley showing the spatial distribution of GFAP (red) and neurofilament (green) at the microelectrode brain tissue interface 2 weeks after implantation (upper panel-A). (B-lower panel) Same section showing the pattern of neurofilament immunoreactivity alone (GFAP signal removed). Notice the loss of signal where up-regulation of GFAP is located immediately surrounding the electrode tract. The base of the letters is 100 microns.



U13-3: Quantitative analysis (N=8) of averaged GFAP immuno reactivity (upper graph) and Neurofilament immunoreactivity (lower graph) as a function of distance from the implant interface. All data from each image used for measurements were normalized to the corresponding intensity in the contralateral or uninjured hemisphere. Hence, a relative

intensity of 0 is normal. The pattern is similar to that observed in the Fisher rat brain indicating that the observation is most likely a general feature of the brain tissue response to implanted silicon microelectrode arrays.



U13-4: Representative horizontal section through the microelectrode tract in motor cortex of young adult male Sprague Dawley showing the spatial distribution of ED-1(red) at the microelectrode brain tissue interface 2 weeks after implantation (upper panel-A). (B-lower panel) Same section showing the pattern of NeuN immunoreactivity (GFAP signal

removed). Notice the loss of signal where up-regulation of ED-1 is located immediately surrounding the electrode tract. The base of the letters is 100 microns.